



BEST DESIGN FOR A FASTEST CELLS SELECTING PROCESS

Michel Pierre, Grégory Vial

► To cite this version:

Michel Pierre, Grégory Vial. BEST DESIGN FOR A FASTEST CELLS SELECTING PROCESS. Discrete and Continuous Dynamical Systems - Series S, 2011, 4 (1), pp.223-237. 10.3934/dcds.2011.4.223 . hal-00461960

HAL Id: hal-00461960

<https://hal.science/hal-00461960>

Submitted on 8 Mar 2010

HAL is a multi-disciplinary open access archive for the deposit and dissemination of scientific research documents, whether they are published or not. The documents may come from teaching and research institutions in France or abroad, or from public or private research centers.

L'archive ouverte pluridisciplinaire **HAL**, est destinée au dépôt et à la diffusion de documents scientifiques de niveau recherche, publiés ou non, émanant des établissements d'enseignement et de recherche français ou étrangers, des laboratoires publics ou privés.

BEST DESIGN FOR A FASTEST CELLS SELECTING PROCESS

MICHEL PIERRE AND GRÉGOR VIAL

IRMAR, ENS Cachan Bretagne, CNRS, UEB
av Robert Schuman F-35170 Bruz, France

(Communicated by the associate editor name)

ABSTRACT. We consider a cell sorting process based on negative dielectrophoresis. The goal is to optimize the shape of an electrode network to speed up the positioning. We first show that the best electric field to impose has to be radial in order to minimize the average time for a group of particles. We can get an explicit formula in the specific case of a uniform distribution of initial positions, through the resolution of the Abel integral equation. Next, we use a least-square numerical procedure to design the electrode's shape.

1. Introduction. We are interested in a mathematical model arising in the optimization of a microsystem, built out of a network of electrodes and whose purpose is to select various living cells, cf [5, 7, 4]. The process is based on the so-called *dielectrophoresis*. When placed in a *nonuniform* electric field, cells become unsymmetrically ionized so that they receive an electric force which makes them move. This may be used to drive cells in a priori chosen places and to select them according to their specificity.

Typically, the network of electrodes has a 2-d periodic structure (see Figure 1) and is placed at the bottom of a thin 3-d device (see Figure 4 page 10). The cells are placed in a liquid medium so that they be driven by electric forces down to the small wells between the electrodes.

The force induced on a cell is proportional to the gradient of the electric field, see [8, 9, 6]. More

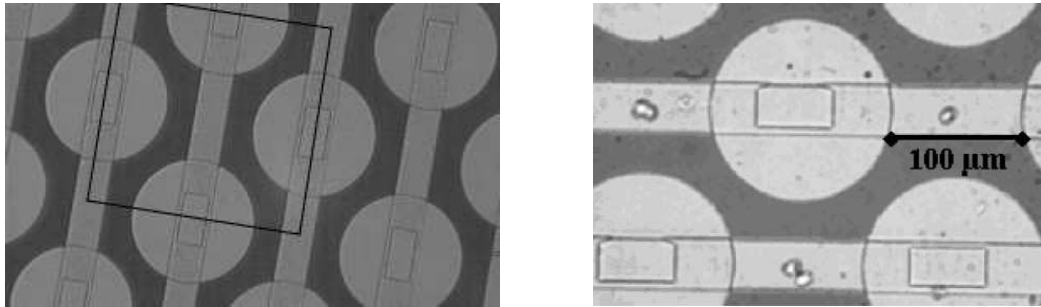


FIGURE 1. Circular electrode network (left: periodic pattern, right: after cell placement).

precisely, a spherical cell of radius r , in a liquid of permittivity ϵ_m , and under the action of an electric field of magnitude E , is submitted to a force

$$\mathbf{F} = 2\pi\epsilon_m r^3 \mathcal{R}[K] \nabla(E^2),$$

where the real part $\mathcal{R}[K]$ of K (called *Clausius-Mosotti factor*) may be positive or negative. In case where $\mathcal{R}[K] < 0$ – *negative dielectrophoresis* – cells move toward the point where the field is minimum. If $U(t)$ denotes the position of a cell at time t , it will move according to the law

$$U''(t) = \mathbf{F} + \Theta = -k\nabla E^2(U(t)) + \Theta(U'(t)), \quad (1)$$

2000 *Mathematics Subject Classification.* 45E10, 49K, 49M, 70B05.

Key words and phrases. optimal design, calculus of variations, numerical optimization, integral equation, dielectrophoresis, kinematics of a particle.

where k is a strictly positive constant in the case of negative dielectrophoresis, and $\Theta = \Theta(U')$ takes into account the friction forces (which are always present in the experiments under consideration).

We want to **control the shape of the electrodes** so that the cells arrive *as fast as possible* to the point where E^2 reaches its minimum. The network of electrodes is assumed to be periodic.

Our strategy is as follows: we first determine what should be the “best” attracting field E *independently of any constraint*: this is essentially a control problem for a family of evolution systems which is mathematically interesting for itself. Then, we try to optimize the shape of the electrodes in order to be as close as possible to this “best” field. According to the law (1), the first step consists in finding the “best” scalar function E^2 so that the solutions $U(t)$ of (1), starting with zero velocity, reach the point where E^2 is minimum (say the origin) *as fast as possible*.

A first helpful reduction is the following (see Section 2.1 for a proof): let x_0 be a starting position for a single particle with initial velocity zero. Given an attracting potential $F = E^2$, one can always replace it by a **radial attracting field** of at most the same size, which will make the particle reach the origin in a shorter time. It is well known that the shortest path to reach a point in \mathbb{R}^3 is a straight line; however, it is not always the “fastest” as it is well known in many situations. We prove in Section 2.1 that it is actually the case here. This is why we will mainly consider radial potentials later on in this paper.

A next question is the following: what is the **best radial** attracting potential to bring a particle the fastest possible from its initial position x_0 to the origin? Actually, it is easy to see (cf. Section 2.1) that the answer will strongly depend on the starting point x_0 . Since we are more interested in *accelerating a group of particles* with a same electric field, we will rather minimize the *average time* necessary for a distributed group of particles to reach the origin. This question is analyzed in Section 3. We prove existence and uniqueness of a best scalar field E^2 . Surprisingly, the question leads to integral equations, one of them being well-known in the literature as the Abel integral equation – see (24).

Next, we will try to design the “fastest shapes” of the electrodes by being as close as possible to the previously obtained “best” radial attracting field. We use a least square method and the objective function to be minimized is an euclidian distance between the expected field and the “best” field found before. This is analyzed numerically in Section 4.

2. Towards the optimization problem.

2.1. Reduction to radial fields. As stated in the introduction, we prove here that one can always do better (= faster) with radial fields. We will essentially discuss the case when $\Theta \equiv 0$ (no friction). As explained in § 2 and Theorem 2.2, it is not difficult to modify the analysis so as to include this term. But the analysis is less technical without it and easier to read while nothing of the essential part is lost.

We denote by $|\cdot|$ the euclidian norm in \mathbb{R}^N . Let $F : \mathbb{R}^N \setminus \{0\} \rightarrow [0, +\infty)$ be a \mathcal{C}^2 -function with ∇F bounded in a neighborhood of the origin 0 and $F(0) := \lim_{|r| \rightarrow 0} F(r) = 0$. Let us consider the solution of

$$U''(t) = -\nabla F(U(t)), \quad U(0) = x_0, \quad U'(0) = 0. \quad (2)$$

This solution exists globally in time since: $|U'|^2 = 2[F(x_0) - F(U)] \leq 2F(x_0)$. We assume that $U(T) = 0$ for some $T > 0$ and we set $e_0 := x_0/|x_0|$.

Theorem 2.1. *There exists $t_0 \in [0, T)$, $\tau \in (t_0, T]$, $G \in \mathcal{C}^1[0, |x_0|]$ and $u \in \mathcal{C}^2([t_0, \tau]; \mathbb{R}^N)$ such that,*

$$\forall t \in (t_0, \tau), \quad u''(t) = -G'(|u(t)|)e_0, \quad u(t_0) = x_0, \quad u'(t_0) = 0, \quad (3)$$

$$G(0) = 0, \quad \|G\|_\infty = G(|x_0|) \leq F(x_0), \quad \|G'\|_\infty \leq \|\nabla F\|_\infty. \quad (4)$$

$$u(\tau) = 0, \quad \text{and } \forall t \in [t_0, \tau], \quad |u(t)| \leq |U(t)|. \quad (5)$$

Remark 1. Let us set: $\forall x \in \mathbb{R}^N, \mathcal{G}(x) = G(|x|)$. Then, for $x \in [0, x_0]$, one has $\nabla \mathcal{G}(x) = G'(|x|)e_0$. This theorem shows that, given x_0 , we may replace the initial potential F by a *radial potential* \mathcal{G} in such a way that the accelerated particle $u(t)$ reaches the origin at least as fast as (and most of the time, faster than) the previous one $U(t)$ and this, with a potential \mathcal{G} “bounded” above by F as well as $\nabla \mathcal{G}$ bounded above by ∇F – see (4).

The dependence in x_0 of this new potential \mathcal{G} is discussed below.

Proof. (of Theorem 2.1) The new radial solution $u(t)$ will be essentially constructed via the orthogonal projection $(U(t) \cdot e_0)e_0$ of $U(t)$ onto the direction of e_0 .

We denote by τ the first time $t \in (0, T]$ such that $U(t) \cdot e_0 = 0$ (we know it exists since $U(T) = 0$). To explain the idea of the proof, we first assume that $U''(t) \cdot e_0 < 0$ for all $t \in (0, \tau)$: this means

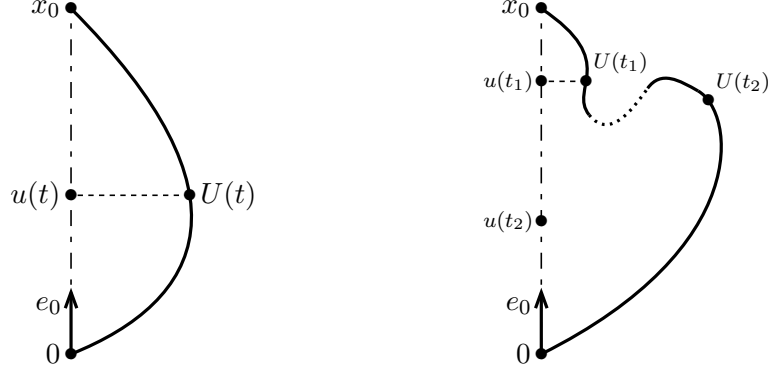


FIGURE 2. Projection onto the e_0 axis (left: monotonic case, right: general case).

that the attraction is directed “downwards” all along the trajectory (assuming e_0 defines the vertical direction, see left picture of Figure 2). Since $U'(0) \cdot e_0 = 0$, this also implies $U'(t) \cdot e_0 < 0$ for all $t \in (0, \tau)$. Then, we set $u(t) = (U(t) \cdot e_0)e_0$. We have, for all $t \in [0, \tau]$

$$u(0) = x_0, |u(t)| = U(t) \cdot e_0, u''(t) = (U''(t) \cdot e_0)e_0 = -[\nabla F(U(t)) \cdot e_0]e_0. \quad (6)$$

Since the mapping $t \in [0, \tau] \rightarrow a(t) = U(t) \cdot e_0 = |u(t)| \in [0, |x_0|]$ is strictly decreasing, we denote by a^{-1} its inverse function (which has the same regularity as a itself). Then, we define $g : [0, |x_0|] \rightarrow [0, +\infty)$ as

$$g(r) = \nabla F(U(a^{-1}(r))) \cdot e_0.$$

And we have, thanks to (6)

$$\forall t \in [0, \tau], \quad u''(t) = -g(|u(t)|)e_0.$$

Note that $g \geq 0$ due to our assumption $U''(t) \cdot e_0 < 0$. We now set $G(r) = \int_0^r g(s)ds$ to obtain Theorem 2.1. By construction $\|G'\|_\infty \leq \|\nabla F\|_\infty$ and, by integration:

$$2[G(|x_0|) - G(|u(t)|)] = |u'(t)|^2 \leq |U'(t)|^2 = 2[F(x_0) - F(U(t))]. \quad (7)$$

And at $t = \tau$, since $u(\tau) = 0$ and $G(|u(\tau)|) = G(0) = 0$, we obtain:

$$|u'(\tau)|^2 = 2G(|x_0|) \leq |U'(\tau)|^2 \leq 2F(x_0), \quad (8)$$

whence the announced estimate on $\|G\|_\infty = G(|x_0|)$.

Henceforth, we consider the general case where it may happen that $U''(t) \cdot e_0 > 0$ for some $t \in (0, T)$ (this is the case of the dashed part of the trajectory in the right picture of Figure 2), that is to say, the attraction is directed upwards at some places on the trajectory. Then, the idea is to continue going down linearly on the direction of e_0 while this happens. We introduce

$$\forall t \in [0, T], \quad a'(t) = - \int_0^t [U''(s) \cdot e_0]^- ds, \quad a(0) = |x_0|.$$

Then, we define

$$t_0 = \inf\{t \in (0, T]; U''(t) \cdot e_0 < 0\}, \quad \tau = \inf\{t \in (t_0, T]; a(t) = 0\}.$$

Note that τ is well-defined; indeed

$$a'(t) \leq \int_0^t U''(s) \cdot e_0 ds = U'(t) \cdot e_0, \quad \text{which implies } a(t) - |x_0| \leq U(t) \cdot e_0 - |x_0|.$$

Since $U(T) \cdot e_0 = 0$, it follows that $a(t)$ vanishes for some $t \in (t_0, T]$.

Now, $t \in [t_0, \tau] \rightarrow a(t) \in [0, |x_0|]$ is strictly decreasing. We denote by a^{-1} its inverse and we define

$$K = \{t \in [t_0, T]; U''(t) \cdot e_0 \leq 0\}; \forall t \in K, \chi_K(t) = 1, \forall t \in [t_0, T] \setminus K, \chi_K(t) = 0, \quad (9)$$

$$\forall r \in [0, |x_0|], g(r) = \chi_K(a^{-1}(r)) [\nabla F(U(a^{-1}(r))) \cdot e_0]. \quad (10)$$

If we now set $u(t) = a(t)e_0$, we have $u(t_0) = x_0$ and for all $t \in [t_0, \tau]$:

$$u''(t) = a''(t)e_0 = -\chi_K(t) [\nabla F(U(t)) \cdot e_0] = -g(|u(t)|)e_0 = -g(|u(t)|)e_0.$$

Note that $g \geq 0$ and is continuous (this only needs to be checked on the boundary of K , and it is easy). We set $G(r) = \int_0^r g(s)ds$ and we finish as in (7)–(8), checking that, here again:

$$G(|u(\tau)|) = 0, \quad 2G(|x_0|) = |u'(\tau)| \leq |U'(\tau) \cdot e_0| \leq |U'(\tau)| \leq 2F(x_0).$$

□

Remark 2. : Case of friction. Assume there is friction in the movement of the cells (which is actually always the case). In this situation, instead of (2), the evolution of each cell is given by

$$U''(t) = -\nabla F(U(t)) + \Theta(U'(t)),$$

where $\Theta \in \mathcal{C}^1(\mathbb{R}^N, \mathbb{R}^N)$. Then Theorem 2.1 may be extended as follows:

Theorem 2.2. *There exists $(t_0, \tau) \in [0, T] \times (0, T]$, $G \in W^{1,\infty}[0, |x_0|]$, $h : [0, +\infty) \rightarrow \mathbb{R}$ measurable and bounded and $u \in \mathcal{C}^2([t_0, \tau]; \mathbb{R}^N)$ such that,*

$$a.e. t \in (t_0, \tau), u''(t) = -G'(|u(t)|)e_0 + h(|u'(t)|)e_0, \quad u(t_0) = x_0, \quad u'(t_0) = 0, \quad (11)$$

$$G(0) = 0, \quad \|G'\|_\infty \leq \|\nabla F\|_\infty, \quad \|h\|_\infty \leq \|\Theta\|_\infty, \quad (12)$$

$$u(\tau) = 0, \quad \text{and } \forall t \in [t_0, \tau], \quad |u(t)| \leq |U(t)|. \quad (13)$$

Proof. We just indicate how to modify the proof of Theorem 2.1. We use the same function $a(t)$ defined through the integration of $-[U''(t) \cdot e_0]^-$. The mapping $t \in [t_0, \tau] \rightarrow a(t) \in [0, |x_0|]$ is nonincreasing, where t_0, τ are defined in the same way as in Theorem 2.1. Again, we denote its inverse by a^{-1} and we define K and g as in (9) and (10). Moreover, the mapping $t \rightarrow -a'(t) \in [0, -a'(\tau)]$ is nondecreasing. We denote by β its left-continuous inverse and we define

$$\forall r' \in [0, -a'(\tau)], \quad h(r') = \chi_K(\beta(r')) [\Theta(U'(\beta(r')))) \cdot e_0].$$

It is then easy to check that

$$a''(t) = -g(a(t)) + h(-a'(t)), \quad \text{or } u''(t) = -g(|u(t)|)e_0 + h(|u'(t)|)e_0.$$

□

Remark 3. : Note that u'' remains continuous, but h may be discontinuous. Actually, if it is the case, then $\tau < T$. Nevertheless, we may approximate h (and also g) by more regular functions and the associated solutions still reach the origin in time $\tau + \epsilon < T$.

2.2. Best potential for a single cell. One may ask whether it is still possible to improve the radial potential G in such a way that the corresponding solution reaches the origin even faster. Let us analyze this in the case without friction. Then, it turns out that an easy expression can be obtained for the “reaching” time. Let us write the solution as follows, where $a(t)$ is a scalar function and $G \in \mathcal{C}^2(\mathbb{R}, \mathbb{R})$:

$$a''(t) = -\frac{1}{2}G'(a(t)), \quad a(0) = a_0 > 0, \quad a'(0) = 0.$$

(We added a factor $1/2$ in the notation only to simplify further expressions). Since we want to accelerate the particle towards $a(\cdot) = 0$, it is better to assume that $G' \geq 0$ (as it is the case in the G obtained in Theorem 2.1 above). This may be integrated as

$$a'^2(t) = G(a_0) - G(a(t)) \quad \text{or} \quad -a'(t) = \sqrt{G(a_0) - G(a(t))}.$$

Let us denote by $\tau(a_0)$ the first time t such that $a(t) = 0$ (assuming it exists). Then integrating once more the above identity, from 0 to $\tau(a_0)$, leads to (note that $a'(t) \leq 0$)

$$\tau(a_0) = \int_0^{\tau(a_0)} \frac{-a'(t)}{\sqrt{G(a_0) - G(a(t))}} dt = \int_0^{a_0} \frac{da}{\sqrt{G(a_0) - G(a)}}. \quad (14)$$

Minimizing $\tau(a_0)$ in this context leads to the following minimization problem: we set

$$\mathcal{H} = \{H \in W^{1,\infty}(0, a_0); H' \geq 0, H(0) = 0, \|H\|_\infty \leq \|G\|_\infty, \|H'\|_\infty \leq \|G'\|_\infty\}.$$

$$\tau_H(a_0) := \int_0^{a_0} \frac{da}{\sqrt{H(a_0) - H(a)}}.$$

And the minimization problem becomes

$$\text{Find } H_{opt} \in \mathcal{H}, \text{ such that } \tau_{H_{opt}}(a_0) = \min\{\tau_H(a_0); H \in \mathcal{H}\}.$$

It is straightforward to check that an optimal H is given by

$$H_m(a) = [G(a_0) + \|G'\|_\infty(a - a_0)]^+.$$

This would be a good optimal solution if we were to deal with only one particle. But we generally want to accelerate several particles together with the same electric field. Since the previous optimal choice depends on a_0 , it is necessary to re-think the optimization process. This is the goal of the next paragraph.

2.3. Best average time for a group of particles. In experiments, one generally wants to accelerate together a whole group of cells located in a region B of the origin, *with the same electric field*. We will assume that B is the ball of radius 1 and centered at the origin.

To take this into account, one idea is to *minimize the average time* taken by the whole set of particles to reach the origin. According to Theorem 2.1, given a potential on B , for each starting point x_0 , we can do better by choosing a radial “modification” of this potential. Therefore, it is natural to look directly for a potential which is directed towards the origin at each point, that is to say, of the form (with $e_0 = x_0/|x_0|$)

$$\mathcal{G}(x_0) = G(x_0)e_0, G : B \rightarrow [0, +\infty), \frac{d}{dr}G(re_0) \geq 0, G(0) = 0. \quad (15)$$

The reaching time of the origin by a particle starting at $x_0 = a_0e_0$ with zero initial velocity is given by (see (14)):

$$\tau_{\mathcal{G}}(x_0) = \tau_{\mathcal{G}}(a_0e_0) = \int_0^{a_0} \frac{da}{\sqrt{G(a_0e_0) - G(ae_0)}}. \quad (16)$$

We denote by $\alpha \in L^1(B)$ the density distribution of the particles at the beginning of the experiment with $\alpha \geq 0, \int_B \alpha(x)dx = 1$. We consider the *minimization of the mean value of the reaching time*, with the weight α , namely

$$\begin{cases} \text{Find } \mathcal{G}_{opt} \text{ minimizing } \int_B \alpha(x_0)\tau_{\mathcal{G}}(x_0)dx_0, \\ \text{among the } \mathcal{G} \text{ as in (15) and with } \|\mathcal{G}\|_\infty \leq A_0, \|\nabla \mathcal{G}\|_\infty \leq A_1, \end{cases}$$

where A_0, A_1 are a priori given bounds (with $A_0 \leq A_1$ since $\mathcal{G}(0) = 0$).

Denoting S^{N-1} the unit sphere in \mathbb{R}^N , the integral to be minimized may be rewritten

$$\int_{S^{N-1}} de_0 \int_0^1 \alpha(a_0e_0)da_0 \int_0^{a_0} \frac{da}{\sqrt{G(a_0e_0) - G(ae_0)}}.$$

Minimizing this integral is equivalent to minimize, **for each** e_0 , the expression

$$T(y) = \int_0^1 \beta(a_0)da_0 \int_0^{a_0} \frac{da}{\sqrt{y(a_0) - y(a)}}, \quad (17)$$

where $\beta(a_0) = \alpha(a_0e_0), y(a) = G(ae_0)$. This is the purpose of next Section.

3. Best potential; the Abel integral equation. As suggested in the previous section, we consider the “reaching time” functional

$$T(y) = \int_0^1 \beta(a_0) da_0 \int_0^{a_0} \frac{da}{\sqrt{y(a_0) - y(a)}} \leq +\infty, \quad (18)$$

where $\beta \in L^1(0, 1)$, $\beta \geq 0$ and $y \in \mathcal{M}$ where

$$\mathcal{M} = \{y : [0, 1] \rightarrow [0, 1] \text{ nondecreasing, } y(0) := \lim_{a \rightarrow 0} y(a) = 0, y(1) := \lim_{a \rightarrow 1} y(a) = 1\}.$$

The choice of $y(1) = 1$ is only a normalization (more generally, we would work with $y/\|y\|_\infty$). Note that a function $y \in \mathcal{M}$ is not well defined at its discontinuity points. But they form an at most countable set so that the integral $T(y)$ is well defined.

We consider the minimization problem

$$y^* \in \mathcal{M}, \quad T(y^*) = \min\{T(y); y \in \mathcal{M}\}. \quad (19)$$

We have a first result.

Proposition 1. *There exists y^* solution of (19). When $\beta > 0$ a.e. on a neighborhood of 1, then it is “unique” (more precisely, two solutions are equal except for their values at their discontinuity points). If $\beta > 0$ a.e., then y^* is strictly increasing.*

Proof. Note that if $y(x) = x$, then $T(y) = \int_0^1 2\beta(a_0)\sqrt{a_0} da_0 < +\infty$, so that $I = \inf\{T(y); y \in \mathcal{M}\} < +\infty$.

Let $(y_n)_{n \geq 1} \in \mathcal{M}$ be such that $T(y_n)$ converges to I . Since the y_n ’s are nondecreasing and bounded, we may assume, up to a subsequence, that they converge a.e. to a nondecreasing function $y^* : [0, 1] \rightarrow [0, 1]$. By Fatou’s Lemma, we have $T(y^*) \leq I$.

It remains to check the boundary conditions $y^*(0) = 0, y^*(1) = 1$: it will follow that $y^* \in \mathcal{M}$ and is a minimum for (19). First, y^* cannot be a constant function since it would make $T(y^*) = +\infty$. Next, we notice that, if $z = [y^* - y^*(0)]/[y^*(1) - y^*(0)]$, we have $z \in \mathcal{M}$ and

$$I \leq T(z) = \sqrt{y^*(1) - y^*(0)} T(y^*) = \sqrt{y^*(1) - y^*(0)} I.$$

This proves $y^*(1) - y^*(0) = 1$, whence the expected boundary conditions.

For the uniqueness, let us work with the representation of y^* which is right-continuous on $[0, 1]$. We remark that $y \rightarrow T(y)$ is convex for all β , and even strictly convex if $\beta > 0$ a.e. on a neighborhood of 1, as one can easily check using the strict convexity of the function $r \rightarrow \frac{1}{\sqrt{r}}$: whence the uniqueness of the minimum of $T(\cdot)$.

Assume now $\beta > 0$ a.e.: if y^* was constant on some interval, we would have $T(y^*) = +\infty$ which is a contradiction; thus, y^* is strictly increasing. \square

Computation of the optimal solution y^* : It is elementary to write down an optimization algorithm to compute y^* (remember that the functional $y \rightarrow T(y)$ is convex). We used here a fixed step gradient method based on a linear discretization. Figure 3 shows the results obtained for several values of β . The only numerical point to worry about is the fact that y^* may be constant (or almost constant) at some places. For instance, we may check that

$$(\beta = 0 \text{ on } [0, \alpha]) \implies (y^* = 0 \text{ on } [0, \alpha]). \quad (20)$$

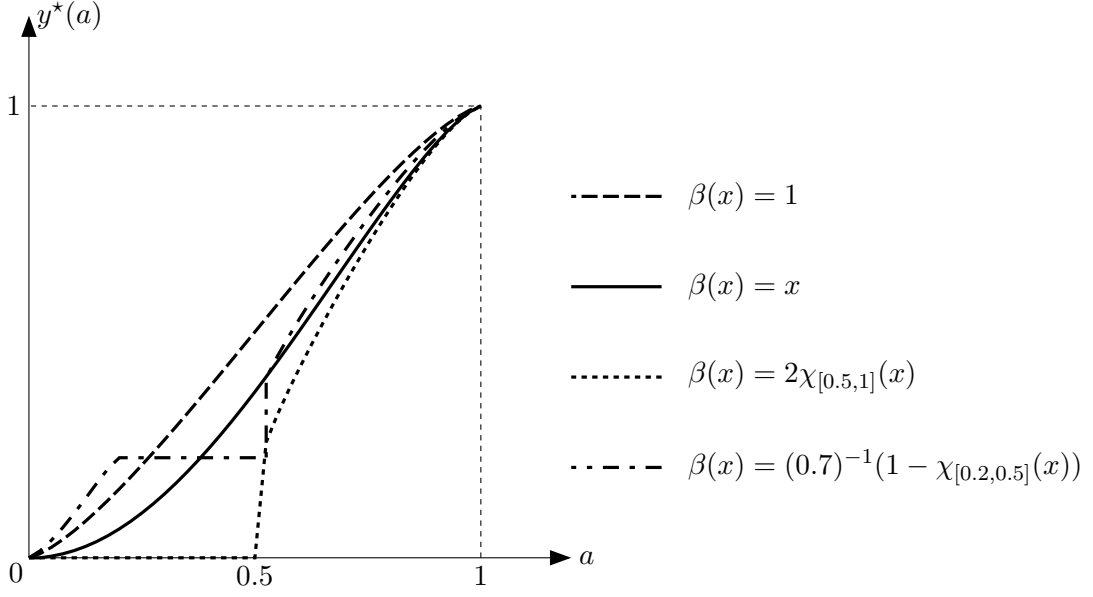
Indeed, we may then write

$$T(y) = \int_\alpha^1 \beta(a_0) da_0 \left[\int_0^\alpha \frac{da}{\sqrt{y(a_0) - y(a)}} + \int_\alpha^{a_0} \frac{da}{\sqrt{y(a_0) - y(a)}} \right].$$

Obviously, given y , if one replaces it by \tilde{y} which equal to zero on $[0, \alpha]$ and equal to y on $[\alpha, 1]$, we have $T(\tilde{y}) \leq T(y)$.

We denote by T_β the reaching time functional associated with a given distribution β , and by y_β^* the corresponding optimal solution. In Table 1, we compare the times $T_\beta(y)$ for various β and y . For $\beta = \beta_1 \equiv 1$, the computations are explicit, while they result from a numerical method with 50 discretization points otherwise.

Analysis of y^* : It turns out that the analysis of the optimal solution y^* is not so easy. In particular, we do not know exactly its regularity. We are able to write down the Euler-Lagrange

FIGURE 3. Optimal solutions y^* obtained for different β .

y	$y_{\beta_1}^*$	$x \mapsto x$	$x \mapsto x^2$
$T_{\beta_1}(y)$	$\frac{\pi^{3/2}}{2\sqrt{2}\Gamma(3/4)^2} \simeq 1.31$	$\frac{4}{3} \simeq 1.33$	$\frac{\pi}{2} \simeq 1.57$
y	$y_{\beta_2}^*$	$x \mapsto x$	y_{β_1}
$T_{\beta_2}(y)$	1.43	1.72	1.67
y	$y_{\beta_3}^*$	$x \mapsto x$	y_{β_1}
$T_{\beta_3}(y)$	1.36	1.40	1.39

TABLE 1. Reaching times for $\beta_1 \equiv 1$, $\beta_2 = 2\chi_{[0.5,1]}$ and $\beta_3 = (0.7)^{-1}(1 - \chi_{[0.2,0.5]})$.

equation (or optimality condition) in general (see Proposition 2 below). But, it is not easy to exploit it, even in the case $\beta \equiv 1$. Actually, in this specific case, the optimality condition can be reformulated in a different way: this is done in Proposition 3. Surprisingly, this leads to an integral equation, with unknown function (or more precisely measure) $\mu(a) = \frac{d}{da}[y^*]^{-1}(a)$, which is rather well known and widely studied in the literature (sometimes called Abel equation, see for instance the paper [2] or the books [1, Chap. 7], [10] on this subject). Using these results, we deduce an explicit expression for y^* in this case (which allows to confirm the computations above). These properties of y^* are summarized in the next two propositions.

Proposition 2. *Let y^* be an optimal solution as in Proposition 1 and let $\nu = \frac{d}{dx}y^*$ (which is a nonnegative measure of mass 1). Then*

$$\nu - a.e. \xi, \quad H(\xi) := \int_0^\xi da \int_\xi^1 \beta(a_0)[y^*(a_0) - y^*(a)]^{-3/2} da_0 = T(y^*). \quad (21)$$

Proposition 3. Assume $\beta \equiv 1$. Then, the optimality condition also reads

$$\forall x \in (0, 1), \quad \int_0^1 \frac{da}{\sqrt{|x - y^*(a)|}} = 2T(y^*) = \int_0^1 \frac{d\mu^*(t)}{\sqrt{|x - t|}}, \quad (22)$$

where $\mu^* = \frac{d}{dt}[y^*]^{-1}$. Its unique solution is given by

$$\mu^*(t) = k [t(1-t)]^{-1/4} dt \text{ where } k = \left[\int_0^1 [t(1-t)]^{-1/4} dt \right]^{-1} = \frac{\sqrt{\pi}}{2\Gamma(\frac{3}{4})^2}. \quad (23)$$

Remark 4. By Proposition 1, we know that y^* is strictly increasing. As a consequence, its inverse function $z^*(t) = [y^*]^{-1}(t)$ is continuous, nondecreasing on $[0, 1]$. Its derivative $\mu^* = \frac{d}{dt}z^*$ is a nonnegative measure without atoms. The above theorem claims that $\mu^* = \hat{k}\lambda$ where λ is the unique solution of the following so-called *Abel integral equation with constant limits of integration* among the nonnegative measures:

$$\forall x \in [0, 1], \quad \int_0^1 \frac{d\lambda(t)}{\sqrt{|x - t|}} = 1. \quad (24)$$

The constant \hat{k} is adjusted so that $\int_0^1 d\mu^* = 1$. It turns out that the solution of (24) is explicitly known as being $t \rightarrow [\pi\sqrt{2}]^{-1}[t(1-t)]^{-1/4}$. For convenience, this is proved completely below, but this exact expression was essentially “guessed” from various results in [2, 3, 1, 10]. It follows also that $T(y^*) = \frac{\pi^{3/2}}{2\sqrt{2}\Gamma(3/4)^2}$.

Proof. (of Proposition 2) It is a priori not clear that $H(\xi)$ is finite for all ξ . We first notice that it is the increasing limit as η decreases to 0 of

$$\eta \in (0, 1) \rightarrow H_\eta(\xi) = \int_0^\xi da \int_\xi^1 \beta(a_0)[(y^*(a_0) - y^*(a)) + \eta]^{-3/2} da_0.$$

In particular, it is lower semi-continuous on $[0, 1]$ since H_η is obviously continuous.

We will use several times the following identity: let λ be a nonnegative measure on $(0, 1)$ with $\int_{(0,1)} d\lambda = 1$ and let Λ be the right-continuous increasing function such that

$$\forall 0 \leq a \leq a_0 \leq 1, \quad \Lambda(a_0) - \Lambda(a) = \int_{(a, a_0]} d\lambda.$$

Then, by Fubini's theorem (note that all functions involved are nonnegative)

$$\int_{(0,1)} H(\xi) d\lambda(\xi) = \int_0^1 da_0 \beta(a_0) \int_0^{a_0} \frac{\Lambda(a_0) - \Lambda(a)}{[y^*(a_0) - y^*(a)]^{3/2}} da \leq +\infty. \quad (25)$$

If $\nu = \frac{d}{da}y^*$, then applying this with $\lambda = \nu$, and using the definition (18) of T , we obtain

$$\int_{(0,1)} H(\xi) d\nu(\xi) = T(y^*). \quad (26)$$

This proves at least that H is finite ν -a.e..

Let now $\psi \in \mathcal{C}[0, 1]$ with $\psi \geq 0$ and $\varphi(x) = \int_0^x \psi(t)dt$. Then, for $t > 0$, the function $(y^* + t\varphi)/(1 + t\varphi(1)) \in \mathcal{M}$ and by minimality of y^* :

$$T(y^*) \leq T\left(\frac{y^* + t\varphi}{1 + t\varphi(1)}\right) = \sqrt{1 + t\varphi(1)} T(y^* + t\varphi). \quad (27)$$

Set $c = y^*(a_0) - y^*(a) \geq 0$ and $d = \varphi(a_0) - \varphi(a) \geq 0$. We have

$$T(y^*) - T(y^* + t\varphi) = \int_0^1 \beta(a_0) da_0 \int_0^{a_0} \frac{t d da}{\sqrt{c(c+td)}[\sqrt{c} + \sqrt{c+td}]}, \quad (28)$$

and by (27), this is bounded above by $T(y^* + t\varphi)[\sqrt{1 + t\varphi(1)} - 1]$. Dividing this inequality by $t > 0$ and letting t tend to zero yield:

$$\int_0^1 \beta(a_0) da_0 \int_0^{a_0} \frac{d da}{c^{3/2}} \leq \varphi(1)T(y^*). \quad (29)$$

In particular, the integral on the left hand-side is finite. Plugging $d = \int_a^{a_0} \psi(\xi) d\xi$, and using (25), this may also be written

$$\int_0^1 \psi(\xi) H(\xi) d\xi \leq \varphi(1) T(y^*) = \int_0^1 \psi(\xi) T(y^*) d\xi.$$

By arbitrariness of ψ , this implies: $H(\xi) \leq T(y^*)$ a.e. $\xi \in (0, 1)$. Since H is lower semi-continuous, the set $\{\xi \in (0, 1); H(\xi) > T(y^*)\}$ is open; being of Lebesgue-measure zero, it is empty. Therefore, $H(\xi) \leq T(y^*)$ for all $\xi \in (0, 1)$. Combined with (26), this implies the expected equality (21). \square

Remark 5. : Since we do not have any a priori regularity for y^* , we cannot say anything about the structure of the measure ν . It may a priori contain singular parts, orthogonal to the Lebesgue measure, or Dirac masses, since even the continuity of y^* is not clear in general.

Proof. (of Proposition 3) Let $\mu(t) = [t(1-t)]^{-1/4}$. Let us prove successively that

$$\left[x \in [0, 1] \rightarrow \int_0^1 \frac{d\mu(t)}{\sqrt{|x-t|}} \text{ is constant} \right], \quad (30)$$

and, if $z(t) = k \int_0^t d\mu(s)$ where k is such that $z(1) = 1$, then for $y = z^{-1}$

$$\xi \in (0, 1) \rightarrow \int_0^\xi da \int_\xi^1 [y(a_0) - y(a)]^{-3/2} da_0 = \text{constant}. \quad (31)$$

To prove (30), we set

$$I(x) := \int_0^1 \frac{[t(1-t)]^{-1/4} dt}{\sqrt{|x-t|}}, \quad (32)$$

and we make the change of variable $t = (1 + \cos \varphi)/2$, $\varphi \in [0, \pi]$; then

$$I(x) = J(\theta) = \int_0^\pi F\left(\frac{\sin \varphi}{|\cos \theta - \cos \varphi|}\right) d\varphi,$$

with $\cos \theta = 2x - 1$ ($\theta \in [0, \pi]$), and $F(r) = \sqrt{r}$. We write

$$J(\theta) = \int_0^\theta F\left(\frac{\sin \varphi}{\cos \varphi - \cos \theta}\right) d\varphi + \int_\theta^\pi F\left(\frac{\sin \psi}{\cos \theta - \cos \psi}\right) d\psi,$$

and we make the following one-to-one changes of variables, respectively in each integral

$$u = \frac{\sin \varphi}{\cos \varphi - \cos \theta}, \quad u = \frac{\sin \psi}{\cos \theta - \cos \psi}. \quad (33)$$

This gives

$$J(\theta) = \int_0^{+\infty} F(u) \varphi'(u) du - \int_0^{+\infty} F(u) \psi'(u) du. \quad (34)$$

But, the two functions $\varphi(u), \psi(u)$ defined in (33) are such that

$$\frac{1}{u} = \frac{\cos \varphi - \cos \psi}{\sin \varphi + \sin \psi} = -\tan\left(\frac{\varphi - \psi}{2}\right),$$

so that $\varphi'(u) - \psi'(u) = 2[1 + u^2]^{-1}$ is independent of θ . It follows from the expression (34) that $J(\theta)$ is also independent of θ .

Let us now prove (31). By making the change of variable $t = y(a) \Leftrightarrow a = z(t)$, we have

$$\int_0^1 \frac{k d\mu(t)}{\sqrt{|x-t|}} = \int_0^1 \frac{da}{\sqrt{|x-y(a)|}}.$$

We will compare the derivative of this function with the derivative of the function involved in (31). But, we first “regularize” them as follows: for $\eta > 0$, we denote

$$G_\eta(x) = \int_0^1 \frac{da}{\sqrt{|x-y(a)| + \eta}}, \quad H_\eta(\xi) = \int_0^\xi da \int_\xi^1 \frac{da_0}{[y(a_0) - y(a) + \eta]^{3/2}}.$$

Then

$$2G'_\eta(x) = \int_0^1 \frac{-\text{sign}(x-y(a)) da}{[|x-y(a)| + \eta]^{3/2}},$$

$$H'_\eta(\xi) = \int_\xi^1 \frac{da_0}{[y(a_0) - y(\xi) + \eta]^{3/2}} - \int_0^\xi \frac{da}{[y(\xi) - y(a) + \eta]^{3/2}}.$$

We have $2G'_\eta(y(\xi)) = H'_\eta(\xi)$, which implies that for all $\psi \in \mathcal{C}_0^\infty(0, 1)$:

$$-\int_0^1 \psi'(\xi) H_\eta(\xi) d\xi = \int_0^1 2G'_\eta(y(\xi)) \psi(\xi) d\xi = \int_0^1 2G'_\eta(x) \psi(z(x)) z'(x) dx. \quad (35)$$

As η decreases to zero, the function G_η increases to the function G_0 which is constant by (30): therefore, its derivative converges to zero in the sense of distributions on $(0, 1)$. We deduce that the integrals in (35) tend to zero (note that $\psi(z(\cdot))z'(\cdot) \in \mathcal{C}_0^\infty(0, 1)$): this says that H'_η converges to 0 in the sense of distributions and this implies (31).

To end the proof of Proposition 3, note that the constant in (31) is necessarily equal to $T(y)$ since, $\int_0^1 \frac{d}{d\xi} y(\xi) H_0(\xi) d\xi = T(y)$ (see the computations (25)–(26) where we replace y^* by y). Then it follows that y satisfies the first order optimality condition of Proposition 2. By strict convexity of $y \in \mathcal{M} \rightarrow T(y)$, we deduce that $y = y^*$. Indeed, according to the convexity of $T(\cdot)$ and to the computations (28), (29), we may write for all $y \in \mathcal{M}$:

$$T(y^*) - T(y) \geq \frac{d}{dt} \Big|_{t=0} T((1-t)y + ty^*) = \int_0^1 da_0 \int_0^{a_0} da \frac{(y^* - y)(a_0) - (y^* - y)(a)}{[y(a_0) - y(a)]^{3/2}},$$

and by (25)

$$T(y^*) - T(y) \geq \int_0^1 \frac{d}{d\xi} [y^* - y](\xi) H_0(\xi) d\xi = T(y) \int_0^1 \frac{d}{d\xi} [y^* - y](\xi) d\xi = 0.$$

Whence $T(y) = T(y^*)$.

Note also that the constant in (30) is $2T(y)$, since after setting $x = y(a_0)$ and integrating with respect to a_0 , we see that this constant is equal to:

$$\int_{(0,1)^2} \frac{da_0 da}{\sqrt{|y(a_0) - y(a)|}} = \int_0^1 da_0 \int_0^{a_0} \frac{da}{\sqrt{y(a_0) - y(a)}} + \int_0^1 da_0 \int_{a_0}^1 \frac{da}{\sqrt{y(a) - y(a_0)}} = 2T(y).$$

□

4. Numerical shape optimization of the electrodes. The microsystem we aim at designing is composed of a periodic network of interdigitated electrodes, see Figure 1. We will optimize the shape of the electrodes in the box of Figure 4, the whole device being deduced by periodicity. As depicted, the opposite electrodes have the same polarity. Furthermore, the four electrodes have the same shape to enforce symmetry and ensure that the field \mathbf{E} vanishes at the center G of the bottom. Of course, the dielectrophoretic potential $E^2 = \|\mathbf{E}\|^2$ is minimal at G , and we expect the cells to move towards this point.

Our numerical strategy consists in finding the best electrodes to produce a field as close as possible to the optimal field obtained in section 3. Since the methods we used are quite standard, we will only give a brief description and show the simulation results.

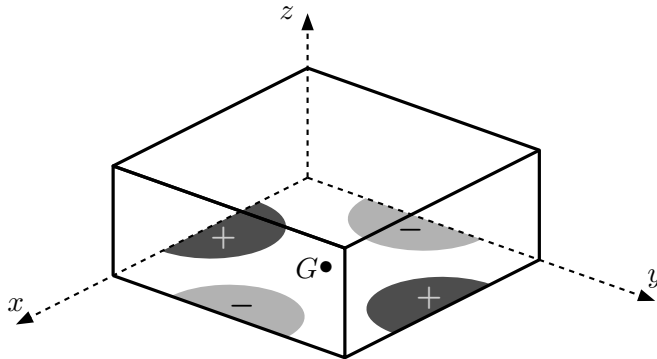


FIGURE 4. Periodic pattern for computations.

4.1. Computation of the electric field for a given shape. Due to the periodicity conditions on the lateral sides of the box, we use a description of the unknowns in terms of Fourier series. Precisely, the electric potential V is written as

$$V(x, y, z) = \sum_{k, \ell \in \mathbb{Z}} V_{k, \ell}(z) e^{i\omega(kx + \ell y)}, \quad (36)$$

with $\omega = 2\pi/L$ where L is the common edge-length in the x and y directions.

The electrodes \mathcal{E}^\pm are supposed to be infinitely thin and are integrated through boundary conditions on $z = 0$. Besides, it is not clear which boundary condition has to be imposed on the top side of the box, and it is more natural to consider a semi-infinite beam with evanescent condition at $z \rightarrow +\infty$. Altogether, the electric potential solves the following Laplace problem:

$$\begin{cases} -\Delta V(x, y, z) &= 0 & \text{for } (x, y, z) \in [0, L] \times [0, L] \times [0, +\infty), \\ V(x, y, 0) &= \pm V_0 & \text{for } (x, y) \in \mathcal{E}^\pm, \\ \partial_z V(x, y, 0) &= 0 & \text{for } (x, y) \notin \mathcal{E}^\pm, \\ V(x, y, z) &\rightarrow 0 & \text{as } z \rightarrow +\infty. \end{cases} \quad (37)$$

The coefficients $V_{k, \ell}(z)$ are given by

$$V_{k, \ell}(z) = V_{k, \ell}(0) e^{-\omega z \sqrt{k^2 + \ell^2}},$$

so that problem (37) reduces to the following linear equation on the $V_{k, \ell}(0)$:

$$\begin{aligned} \sum_{k, \ell \in \mathbb{Z}} V_{k, \ell}(0) e^{i\omega(kx + \ell y)} &= \pm V_0 & \text{for } (x, y) \in \mathcal{E}^\pm, \\ \sum_{k, \ell \in \mathbb{Z}} V_{k, \ell}(0) \sqrt{k^2 + \ell^2} e^{i\omega(kx + \ell y)} &= 0 & \text{for } (x, y) \notin \mathcal{E}^\pm. \end{aligned}$$

If the discretization incorporates N Fourier frequencies, a collocation method leads to a full $N \times N$ linear system. The electric potential V is reconstructed via inverse fast Fourier transform, as well as the electric field

$$\mathbf{E} = -\nabla V.$$

4.2. Least square optimization. The optimal electric field being determined according to Section 3, we now design the electrodes to produce the closest field in a least square sense. As mentioned above, we force the electrodes to be identical (another symmetry axis is also imposed in the computations below). We start from circular shapes – which were already considered to be the best shapes from an experimental point of view, among those considered in [4]. Then, we apply a descent method for the optimization criterion:

$$\text{Find } E \text{ minimizing } \|E - E^*\|^2 = \int_{\Omega} (E - E^*)^2(x, y) dx dy, \quad (38)$$

where the target field E^* is given in Section 3 and where Ω is a region of interest around the origin in the horizontal section $z = 1/30$ which corresponds to experimental initial positions of the cells (note that choosing the whole box for Ω would not be very relevant since the field produced by planar electrodes does certainly have a completely non-radial structure).

The electrodes are represented by a spline interpolation of *control points*. Figure 5 shows the electrodes obtained with 5 such points after the optimization process (the procedure consists in a periodic relaxation among boundary deformations of the electrodes along the normal vector at each control point).

We may compare the average time of a particle to reach the minimum of the field for the two situations of Figure 5. A Monte-Carlo method coupled with the numerical resolution of the ordinary differential equation (2) attests a gain of about 20% with respect to the best known shapes see [4].

Finally, let us mention that we also applied our optimization algorithm by replacing the least-square objective (38) by the average numerical reaching time. The obtained electrodes are similar to those of Figure 5, with comparable “optimal” reaching times.

Acknowledgements : We thank Bruno LePiouffe and Marie Fr  n  a-Robin for having suggested this nice problem, and Martin Costabel for fruitful discussions around it.

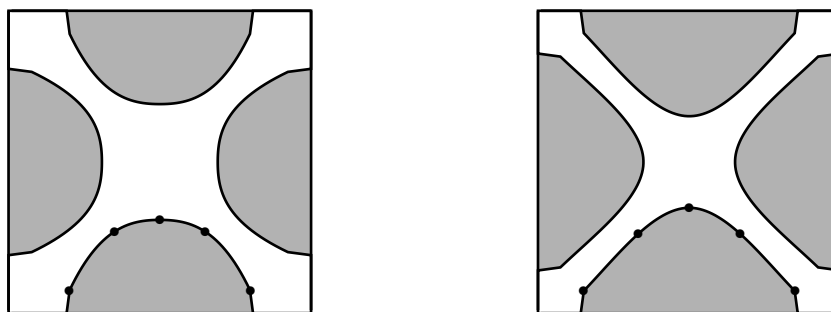


FIGURE 5. Initial circular electrodes (left) and optimized electrodes (right).

REFERENCES

- [1] A. V. BITSADZE. *Integral equations of first kind*, volume 7 of *Series on Soviet and East European Mathematics*. World Scientific Publishing Co. Inc., River Edge, NJ 1995.
- [2] T. CARLEMAN. Über die Abelsche Integralgleichung mit konstanten Integrationsgrenzen. *Math. Z.* **15**(1) (1922) 111–120.
- [3] G. I. ESKIN. *Boundary value problems for elliptic pseudodifferential equations*, volume 52 of *Translations of Mathematical Monographs*. American Mathematical Society, Providence, R.I. 1981. Translated from the Russian by S. Smith.
- [4] M. FRÉNEA, S. P. FAURE, B. L. PIOUFLE, P. COQUET, H. FUJITA. Positioning living cells on a high-density electrode array by negative dielectrophoresis. *Materials Science and Engineering: C* **23**(5) (2003) 597–603.
- [5] Y. HUANG, R. PETHIG. Electrode design for negative dielectrophoresis. *Measurement Science and Technology* **2**(12) (1991) 1142–1146.
- [6] T. JONES. *Electromechanics of Particles*. Cambridge University Press, Cambridge 1995.
- [7] H. MORGAN, M. P. HUGHES, N. G. GREEN. Separation of submicron bioparticles by dielectrophoresis. *Biophysical journal* **77**(1) (1999) 516–525.
- [8] H. A. POHL. The motion and precipitation of suspensoids in divergent electric fields. *Journal of Applied Physics* **22**(7) (1951) 869–871.
- [9] H. A. POHL. *Dielectrophoresis*. Cambridge University Press, Cambridge 1978.
- [10] A. D. POLYANIN, A. V. MANZHIROV. *Handbook of integral equations*. Chapman & Hall/CRC, Boca Raton, FL, second edition 2008.

E-mail address: michel.pierre@bretagne.ens-cachan.fr

E-mail address: gregory.vial@bretagne.ens-cachan.fr